STEM CELLS AND DEVELOPMENT
Volume 28, Number 15, 2019

DOI: 10.1089/scd.2019.0027

MicroRNA-200c Attenuates Periodontitis by Modulating Proinflammatory and Osteoclastogenic Mediators

Adil Akkouch,[1] Min Zhu,[1] Miguel Romero-Bustillos,[2] Steven Eliason,[3,4] Fang Qian,[1] Aliasger K. Salem,[5] Brad A. Amendt,[1,3,4] and Liu Hong[1,3]

This study tested whether microRNA *(miR)-200c* can attenuate the inflammation and alveolar bone resorption in periodontitis by using an in vitro and a rat model. Polyethylenimine (PEI) was used to facilitate the transfection of plasmid DNA encoding *miR-200c* into primary human gingival fibroblasts (HGFs) and gingival tissues of rats. We first analyzed how proinflammatory and osteoclastogenic mediators in HGFs with overexpression of *miR-200c* responded to *Porphyromonas gingivalis* lipopolysaccharide (LPS-PG) challenge in vitro. We observed that overexpression of *miR-200c* significantly reduced interleukin (IL)-6 and 8 and repressed interferon-related developmental regulator-1 *(IFRD1)* in HGFs. *miR-200c* also downregulated *p65* and *p50*. In a rat model of periodontitis induced by an LPS injection at the gingival sulcus of the second maxillary molar (M2), we analyzed how the mediators in rat gingiva and alveolar bone resorption responded to *miR-200c* treatment by a local injection of PEI-plasmid *miR-200* nanoplexes. We observed that the local injection of *miR-200c* significantly upregulated *miR-200c* expression in gingiva and reduced *IL-6, IL-8, IFRD1*, and the ratio of receptor activator of nuclear factor kappa-B ligand/osteoprotegerin. Using micro-computed tomography analysis and histomorphometry, we further confirmed that local treatment with *miR-200c* effectively protected alveolar bone resorption in the rat model of periodontitis by reducing the distance between the cemento-enamel junction and the alveolar bone crest and the inter-radicular space in the upper maxilla at M2. These findings imply that *miR-200c* may serve as a unique means to prevent periodontitis and associated bone loss.

Keywords: alveolar bone loss, proinflammatory, microRNA, periodontitis, polyethylenimine

Introduction

Approximately 50% of adults have been diagnosed with periodontitis in the United States, and periodontitis rates are further increased in aged populations, diabetes patients, and smokers [1–4]. The periodontitis characterized by alveolar bone loss (ABL) is the leading cause of tooth loss among adults [5]. Current treatments to arrest periodontal bone loss, including antiresorptive and anabolic agents, are largely ineffective [6,7]. Further, bisphosphonates as a drug for treating periodontal bone loss has been reported to cause osteonecrosis of jaws as side effects [8]. Bacterially derived factors initiate periodontitis, whereas the imbalance and dysregulation of proinflammatory cytokines, transcription factors, and bone metabolism mediators contribute to the progression of periodontitis and alveolar bone resorption. Specifically, after recognizing periodontal pathogens, Toll-like receptors (*TLRs*) initiate the resistance to the infection by upregulating interleukin *(IL)-6, IL-1β*, and tumor necrosis factor *(TNF)-α* [9,10]. These TLR-mediated proinflammatory cytokines lead to activation of nuclear factor kappa-light-chain-enhancer of activated B cells *(NF-kB)* [11] that, subsequently, amplify the inflammatory response. This upregulated inflammation results in overproduced matrix metalloproteinases and stimulated activities of chemokines [12]. Meanwhile, the migrating cells, including lymphocytes and phagocytes, upregulate receptor activator of nuclear factor kappa-B ligand *(RANKL)*, *TNF-α*, and *IL-17*. The dysregulated proinflammatory factors eventually activate osteoclastogenesis and result in periodontal bone resorption via the *RANKL*/osteoprotegerin (*OPG*) [13]. Managing the imbalance and dysregulation of proinflammatory cytokines and osteoclastogenic mediators has emerged as an effective approach to ameliorate and treat periodontitis and associated bone loss [9,14,15].

MicroRNAs (miRs) are small non-coding RNAs that play critical roles in inflammation, osteogenesis, and osteoclastogenesis and contribute to the pathogenic progression of

[1]Iowa Institute for Oral Health Research and [2]Department of Periodontics, College of Dentistry, The University of Iowa, Iowa City, Iowa.
[3]Center for Craniofacial Anomalies Research and [4]Department of Anatomy and Cell Biology, Carver College of Medicine, The University of Iowa, Iowa City, Iowa.
[5]Department of Pharmaceutical Sciences and Experimental Therapeutics, College of Pharmacy, The University of Iowa, Iowa City, Iowa.

periodontitis [16–18]. *miR-200c* is a member of the *miR-200* family and is significantly under-expressed in gingival tissues of periodontitis patients [17,19]. It regulates multiple signal pathways of proinflammatory factors and represses the expression and activity of *NF-kB* [19–22]. *miR-200c* has also been demonstrated as a tumor suppressor in many types of cancers [23]. Our previous studies have reported that *miR-200c* effectively inhibited *IL-6*, *IL-8*, and chemokine (C-C motif) ligand *(CCL)-5* in human preosteoblasts and periodontal ligament fibroblasts by targeting the *3′UTRs* of these genes [24]. *miR-200c* also improved osteogenic differentiation of preosteoblasts and human bone marrow mesenchymal stem cells. In this study, we tested whether *miR-200c* could be a preventive means for repressing inflammation and attenuating ABL in periodontitis by using human gingival fibroblasts (HGFs) and a rat model of periodontitis induced by *Porphyromonas gingivalis* lipopolysaccharide (LPS-PG) injection [25,26].

Materials and Methods

Construction of miR expression plasmids

The sequence of mature *hsa-miR-200c-3p* (accession number MIMAT0000617) was retrieved from the Ensembl database and mirbase (Integrated DNA Technologies, Coralville, IA). *miR-200c* oligonucleotides that include ~100 bp upstream and 100 bp downstream sequence flanking the ~80 bp stem loop sequence were polymerase chain reaction (PCR) amplified and cloned into pSilencer 4.1 CMV puro vector according to the manufacturer's instructions (Addgene, Cambridge, MA).

Cell culture and transient transfection using polyethylenimine

As the resident cells in periodontitis, primary HGFs (Sciencell, Carlsbad, CA) were used to test the inhibitory function of *miR-200c* in proinflammatory and osteoclastogenic mediators. HGFs were grown in Dulbecco's modified Eagle's medium (DMEM) supplemented with 10% fetal bovine serum, 100 IU/mL penicillin G, and 25 μg/mL streptomycin. For the in vitro transfection of *miR-200c*, plasmid DNA (pDNA) containing *miR-200c* or empty vector (EV) was incorporated into branched polyethylenimine (PEI, MW 25 kDa; Sigma-Aldrich, St. Louis, MO) to form a complex at an *N*/*P* ratio of 10:1 (ratio of the total number of end amine groups (*N*) of PEI and the total number of DNA phosphate groups (*P*) [27]. Briefly, the nanoplexes were prepared by adding 50 μL PEI solution to 50 μL *miR-200c* (10 μg) solution and mixed for 30 s. The mixture was then incubated at room temperature for 30 min to allow nanoplex formation. PEI-*miR-200c* nanoplexes (1, 5, and 10 μg/per well) in 1-mL Opti-MEM were added to HGFs in 6-well plates (10^5 cells/well).

Live/Dead and cell proliferation assay

LIVE/DEAD® assay (Life Technologies, Grand Island, NY) was used to evaluate the cytotoxicity of HGFs treated with PEI-*miR-200c* or PEI-EV nanoplexes. Total cell viability (%) was determined by calculating the percentage of live cells in total cells after 72 h transfection under a fluorescence microscope. A total of four random quadrants were selected from each triplicate for quantification. MTT assay [3-(4,5-dimethylthiazol-2-yl)-2,5-diphenyltetrazolium bromide)] (Life Technologies) was also performed up to 96 h after transfection. The absorbance of optical density (OD) at 540 nm was used to indicate the effect of PEI-*miR-200c* transfection on HGF proliferation and metabolic activity (Sigma-Aldrich).

Effect of miR-200c *on proinflammatory and bone mediators in HGFs*

HGFs with different transfections for 72 h were treated with LPS-PG (1 μg/mL) (InvivoGen, San Diego, CA) for up to 48 h. The transcripts of proinflammatory and bone mediators that potentially participate in periodontitis and associated ABL, including *IL-6*, *IL-8*, interferon-related developmental regulator 1 (*IFRD1*), *NF-kB* subunit *p65, p50, OPG*, and *RANKL* [28], were subsequently quantitated by using real-time PCR. Their protein contents in supernatants or the lysis of the cells were measured by using ELISA (Thermo Fisher Scientific, St Peters, MO). Total RNA and miRs were prepared by using the miRNeasy Mini Kit (Qiagen, Hilden, Germany). *miR-200c* was reverse transcribed by using TaqMan microRNA assay probes and the TaqMan microRNA reverse transcription kit (Applied Biosystems, Austin, TX). Quantitative real-time PCR analysis of miRs was performed by using TaqMan microRNA assay probes and normalized by using the *U6B* probe. The vacuolar protein sorting 29 homolog (*VPS29*) was used as an internal control for human cells [29], whereas the ribosomal protein gene (*RPS18*) was used as reference genes for rat samples [30]. The primers used were included in Table 1.

Effect of miR-200c *on periodontitis in vivo*

The rat model of periodontitis was induced by a microinjection of LPS-PG into the gingival sulcus of 12-week-old male Sprague Dawley rats (Charles River Laboratories) [25,26]. All protocols for animal procedures were approved by the Office of Animal Resources at the University of Iowa. Under the general anesthesia, a total of 48 rats were assigned to six groups to receive different treatments after the introduction of periodontitis: (1) phosphate-buffered saline (PBS) (Sham control); (2) LPS alone; (3) LPS + EV at 1 μg/injection; (4) LPS + EV at 10 μg/injection; (5) LPS + *miR-200c* at 1 μg/injection; and (6) LPS + *miR-200c* at 10 μg/injection. To induce the rat periodontitis, 1 μL of LPS-PG at 10 μg/μL was injected twice a week by using a Hamilton micro-syringe into the gingival sulcus of the second maxillary molar (M2). For the *miR-200c* treatment, different doses of PEI-*miR-200c* at 1 μL were micro-injected into the gingival tissues once a week. Rats were euthanized after 4, 7, and 28 days and samples were collected and analyzed by using real-time PCR, micro-computed tomography (μCT), and histology blindly. The sample size for the collection after 4 and 7 days was 3 and for the collection after 28 days it was 8.

μCT scanning and assessment

The rat maxillae were analyzed by using a high-resolution μCT scanner (Skyscan 1272; Bruker, Aartselaar, Belgium). The scanning protocol was set at an isotropic voxel size of 9.8 μm, and the X-ray energy settings were 80 kV and

Table 1. Sequence for Forward and Reverse Primer Sets Used for Real-Time Polymerase Chain Reaction

Primer	*Forward primer (5′-3′)*	*Reverse primer (5′-3′)*
Human primers		
IL-6	CCATCTTTGGAAGG TTCAGGTTG	ACTCACCTCTTCA GA ACGAATTG
IL-8	AACCCTCTGCACCC AGTTTTC	ACTGAGGATTGA GAGTGGAC
CCL-5	TGCCCACATCAAGG AGTATTT	CTTGCTGTCCCTC TCTCTTTG
IFRD1	TGCAGTGGTTATAG CGATCCT	CCTTGTCTTCGCA CTCTTATCC
P65	CGCTGCTCTAGAGA ACACAATGGCCA CTTGCCG	GCGGCCAAGCTTA AGATCTGCCGA GATAAC
p50	ATGTATGTGAAGGC CCATCC	TTGCTGGTCCCAC ATAGTTG
VPS29	GAATAACTTGGTGT CCGTGGAT	GTGAGAGGAGAC TTCGATGAGA
Rat primers		
IL-6	GCCCTTCAGGAACA GCTATGA	TGTCAACAACATC AGTCCCAAGA
IL-8	CATTAATATTTAAC GATGTGGATGCG TTTCA	GCCTACCATCTTT AAACTGCA CAAT
IFRD1	ATCGGACTGTTCAA CCTTTCAG	GCACTCTTATCAA GGGTTAGGTC
RUNX2	CTTCAAGGTTGTAG CCCTCG	TAGTTCT CATCAT TCCCGGC
ALP	GCAGGATCGGAAC GTCAAT	ATGAGTTGGTAAG GCAGGGTC
RANKL	CCCATCGGGTTCCC ATAAAGTC	GCCTGAAGCAAAT GTTGGCGTA
OPG	GTCCCTTGCCCTGA CTACTCT	GACATCTTTTGCA AACCGTGT
RPS18	GTGATCCCCGAGAA GTTTCA	AATGGCAGTGAT AGCGAAGG

ALP, alkaline phosphatase; CCL, chemokine (C-C motif) ligand; IFRD1, interferon-related developmental regulator-1; IL, interleukin; OPG, osteoprotegerin; RANKL, receptor activator of nuclear factor kappa-B ligand; RPS18, ribosomal protein gene; RUNX2, runt related transcription factor 2; VPS29, vacuolar protein sorting 29 homolog.

125 μA. The scans were reconstructed by using NRecon software (Bruker) to generate three-dimensional models of the rat maxillae. The measurement of ABL consisted of determining the linear distance between the cemento-enamel junction (CEJ) and the alveolar bone crest (ABC) on the interproximal surface of the teeth on the palatal side of the maxilla, with the use of CTAn software (Bruker). The ABL was measured at two points on each M2, which were the mesiobuccal and distobuccal. A higher ABL value implies a more severe bone loss. In addition, the inter-radicular space was measured by using two-dimensional midsagittal sections as the distance from the crest of the inter-radicular bone to the molar root furcation. Next, to investigate the quantity and the quality of the alveolar bone after LPS-PG and miRs treatment, a volume of interest (VOI) was designed as the bone body that encompassed the roots of M2. The VOI length extended from the most mesial to the most distal aspects of the upper M1 and M2 roots, respectively. Its width extended from the most buccal to the most palatal aspect of the M1 or M2 roots, and the height extended from the most apical aspect of the M1 or M2 roots to the most coronal part of the ABC. The percentage of alveolar bone volume/tissue volume (BV/TV), the specific bone surface (BS/BV), the trabecular thickness (Tb. Th), and the total porosity of each sample were measured by using the CTAn software.

Histological analysis

Fixed maxillae were decalcified with 14% EDTA, dehydrated in gradient alcohol, cleared with xylene, and embedded in paraffin. Coronal sections of 7-μm thickness were prepared and stained with hematoxylin and eosin (H&E) and Masson's trichrome. Sections were analyzed and photographed by using an inverted Nikon microscope (Nikon, Japan) followed by a blinded evaluation of bone tissue and collagen fibers of the periodontal ligament region. Analysis of potential alveolar bone-periodontal ligament-cementum defects in the rat periodontitis model was done by using Masson's trichrome staining.

Statistical analysis

Descriptive statistics were conducted, and one-way analysis of variance (ANOVA), followed by the post-hoc Tukey-Kramer test, was used to detect the difference among the experimental groups under different conditions. In addition, the Shapiro-Wilks' test was applied to verify assumption of normality. Statistical analyses were performed by using the statistical package SAS® System version 9.4 (SAS Institute, Inc., Cary, NC), and all tests utilized a 0.05 level of significance.

Results

PEI facilitates the transfection of pDNA encoding miR-200c *in vitro*

After treating HGFs with different doses of the nanoplex of PEI-pDNA carrying *miR-200c* at an *N*/*P* ratio of 10, the level of *miR-200c* transcript was intensely increased in a dose-dependent manner ($P < 0.01$) (Fig. 1A). The cells maintained an elongated and a spindle-shaped form after the treatment. The viability of cells ranged from 95% to 98% by Live/Dead assay, and no difference was observed compared with untreated groups (Fig. 1B, C). In addition, proliferation rate of the cells treated with *miR-200c* at 10 μg/mL was significantly higher than the other treatment groups analyzed by MTT assay (Fig. 1D).

Overexpression of miR-200c *reduced LPS-induced proinflammatory mediators in HGFs in vitro*

LPS-PG at 1 μg/mL strongly upregulated the transcript of *IL-6* (~160-fold) and *IL-8* (~3,700-fold) in control HGFs without treatment, respectively ($P < 0.01$) (Fig. 2A, B). PEI treatment alone had no effect on the *IL-6* and *IL-8* expression, and the HGFs treated with EV slightly increased *IL-6* and *IL-8* transcripts. However, the cells

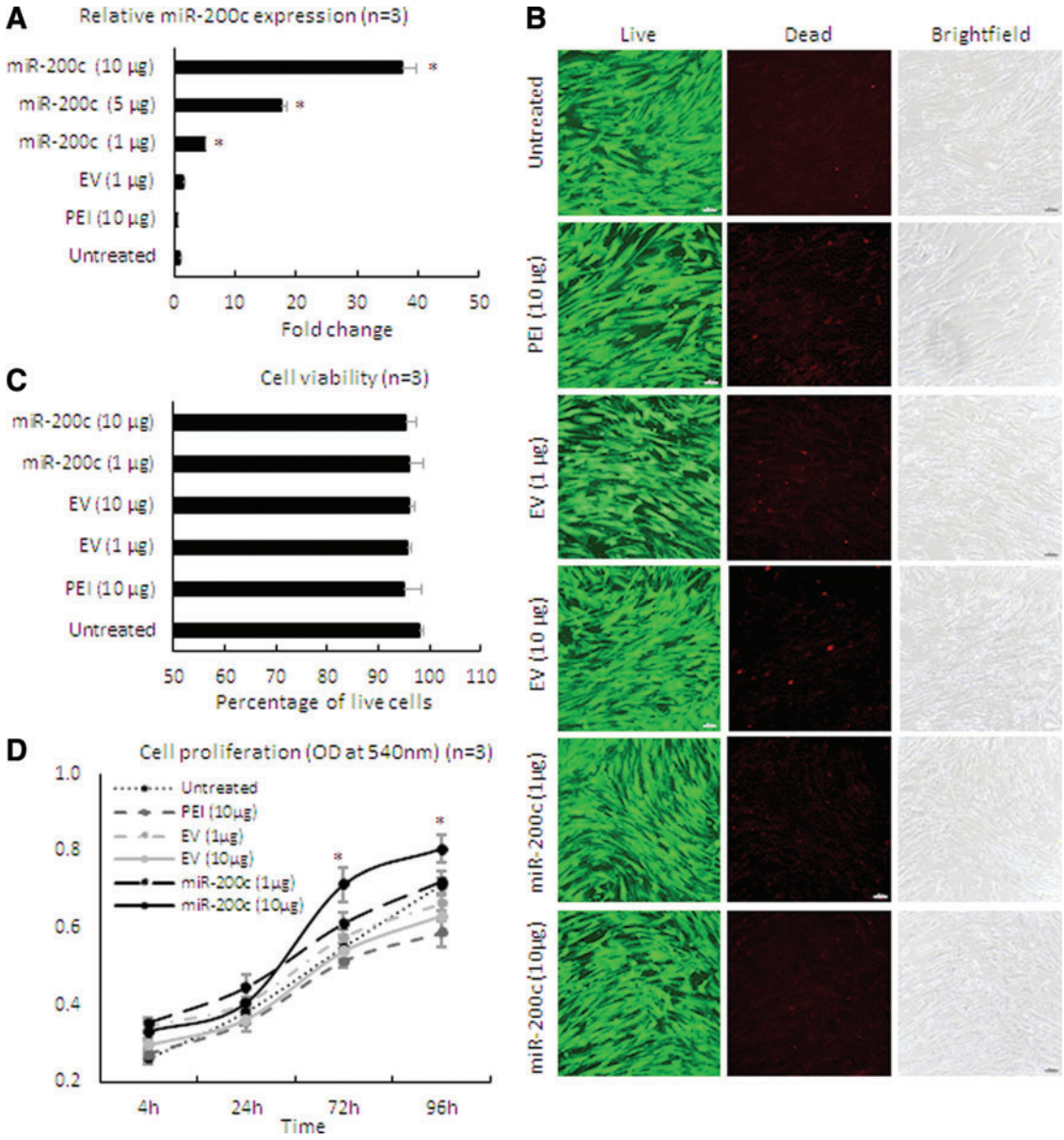

FIG. 1. Cell viability, proliferation, and *miR-200c* expression in HGF cells after transfection with PEI-*miR-200c* nanoplex. **(A)** Fold change of *miR-200c* expression in HGF cells evaluated by quantitative polymerase chain reaction. **(B, C)** Microphotographs of HGFs with Live/Dead staining **(B)** and the percentage of viable cells **(C)** 3 days after transfection with PEI-*miR-200c*. Bars = 100 µm. **(D)** MTT assay [3-(4,5-dimethylthiazol-2-yl)-2,5-diphenyltetrazolium bromide)] results for the HGF 4 days after different treatments; $*P < 0.05$ versus EV (10 µg); performed in replicate. EV, empty vector; IL, interleukin; HGF, human gingival fibroblast; PEI, polyethylenimine. Color images are available online.

treated with *miR-200c* expressed significantly fewer *IL-6* and *IL-8* transcripts than control cells without treatment ($P < 0.05$). The reduction of *IL-6* and *IL-8* transcripts was dose-dependent (Fig. 2A, B). In addition, in LPS-stimulated HGF cells as well as PEI- or EV-treated cells, we found that *IFRD1*, *p65*, and *p50* transcripts were upregulated compared with the untreated control group ($P < 0.05$) (Fig. 2C–E). *miR-200c* transfection followed by LPS challenge showed a significant inhibition of *IFDR1*, *p65* and *p50* transcripts in a dose-dependent manner. Bioinformatic analysis using computational algorithms predicted that *miR-200c* directly targets the *3′UTR* of *IFRD1* mRNA at the position 1,120–1,126 (Fig. 2F) (www.targetscan.com). In addition, LPS challenge significantly increased the protein levels of *IL-6* and *IL-8* measured by using ELISA in the supernatant of culture medium produced by HGF after 24 h ($P < 0.05$) (Fig. 3A, B), which was consistent with their transcripts measured by using real-time PCR. Treatments with PEI and EV did not reduce *IL-6* and *IL-8* levels; however, treatment with *miR-200c* at 5 and 10 µg significantly reduced the levels of *IL-6* and *IL-8* than the groups without treatment or treated with EV and PEI alone ($P < 0.05$). The protein levels of *IFRD1* and *p65* in the lysis of HGFs 24 h after treatment with *miR-200c* at 5 and 10 µg are also significantly lower than the LPS-challenged group without treatment (Fig. 3C, D).

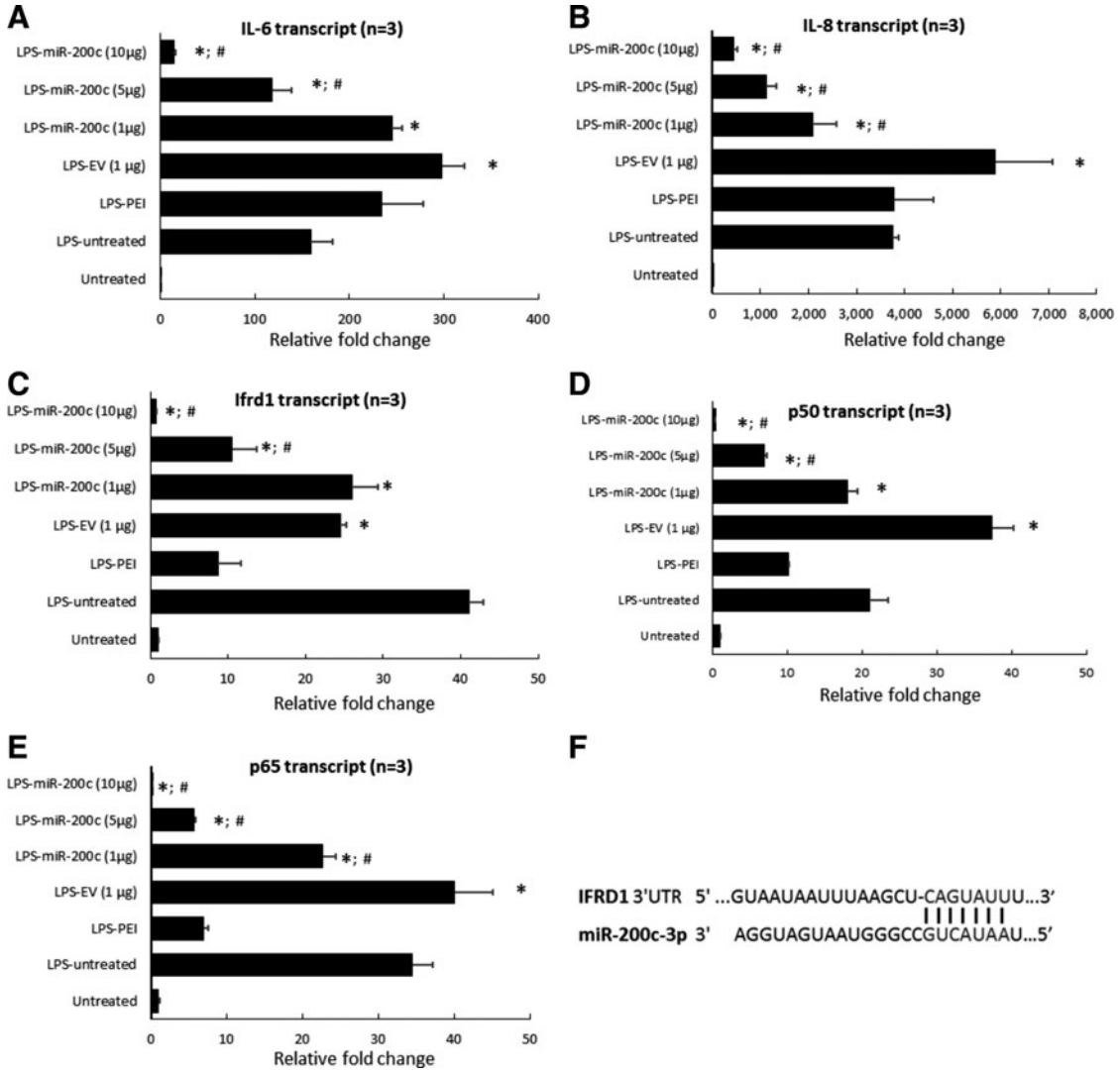

FIG. 2. *miR-200c* reduces protein level of proinflammatory and osteoclastogenic mediators after LPS stimulation. **(A–E)** Relative fold change of transcripts of *IL-6* **(A)**, *IL-8* **(B)**, *p50* **(C)**, *p65* **(D)**, and *IFRD1* **(E)** in HGFs with different transfections 24 h after stimulation with 1 μg/mL of LPS-PG. $^{*}P < 0.05$ versus HGFs untreated with LPS; $^{\#}P < 0.05$ versus LPS-EV; performed in replicate. **(F)** *Targetscan.org* predicted the possible binding site of *miR-200c-p3* and the *3′UTR* of *IFRD1* at the position 1,120–1,126. *IFRD1*, interferon-related developmental regulator-1; LPS-PG, *Porphyromonas gingivalis* lipopolysaccharide.

Transfection of miR-200c *using PEI suppressed proinflammatory mediators of periodontitis in vivo*

Figure 4A summarized the in vivo expression of *miR-200c* after PEI-*miR-200c* nanoplexes were injected into the rat's gingival tissues. We observed a small upregulation of *miR-200c* for groups treated with EV compared with endogenous *miR-200c* of rats without treatment, and returned to control levels after 7 days. However, after 4 days, the *miR-200c* transcript in the gingival tissues treated with *miR-200c* at 1 and 10 μg exhibited ∼135- and 270-fold higher levels, respectively, than did endogenous *miR-200c* in gingival tissue ($P < 0.01$). These transcript levels are also significantly higher than they were for rats receiving EV (10 μg) and PBS ($P < 0.05$). Although the expression of *miR-200c* slightly declined after 7 days, the *miR-200c* maintained significantly higher levels (seven-fold) than did untreated gingiva ($P < 0.05$). An injection of PBS and EV increased *IL-6, IL-8*, and *IFRD1* transcripts after 4 days (Fig. 4B–D). Of particular note, the injection of PEI-*miR-200c* nanoplex at 10 μg significantly downregulated *IL-6, IL-8*, and *IFRD1* ($P < 0.01$), whereas *miR-200c* at a low dose (1 μg) did not repress them. In addition, gingiva receiving an injection of PBS or EV significantly increased the *RANKL/OPG* ratio ($P < 0.05$) than untreated control gingiva (Fig. 4E). However, *miR-200c* treatment significantly downregulated *RANKL/OPG* ratio by decreasing *RANKL* and enhancing *OPG* expression.

miR-200c *prevented ABL in experimental periodontitis of rats*

Figure 5A summarized the μCT images for ABL in rats 4 weeks after receiving an LPS injection and the different miR treatments. Alveolar crest bone (ACB) receded more at the

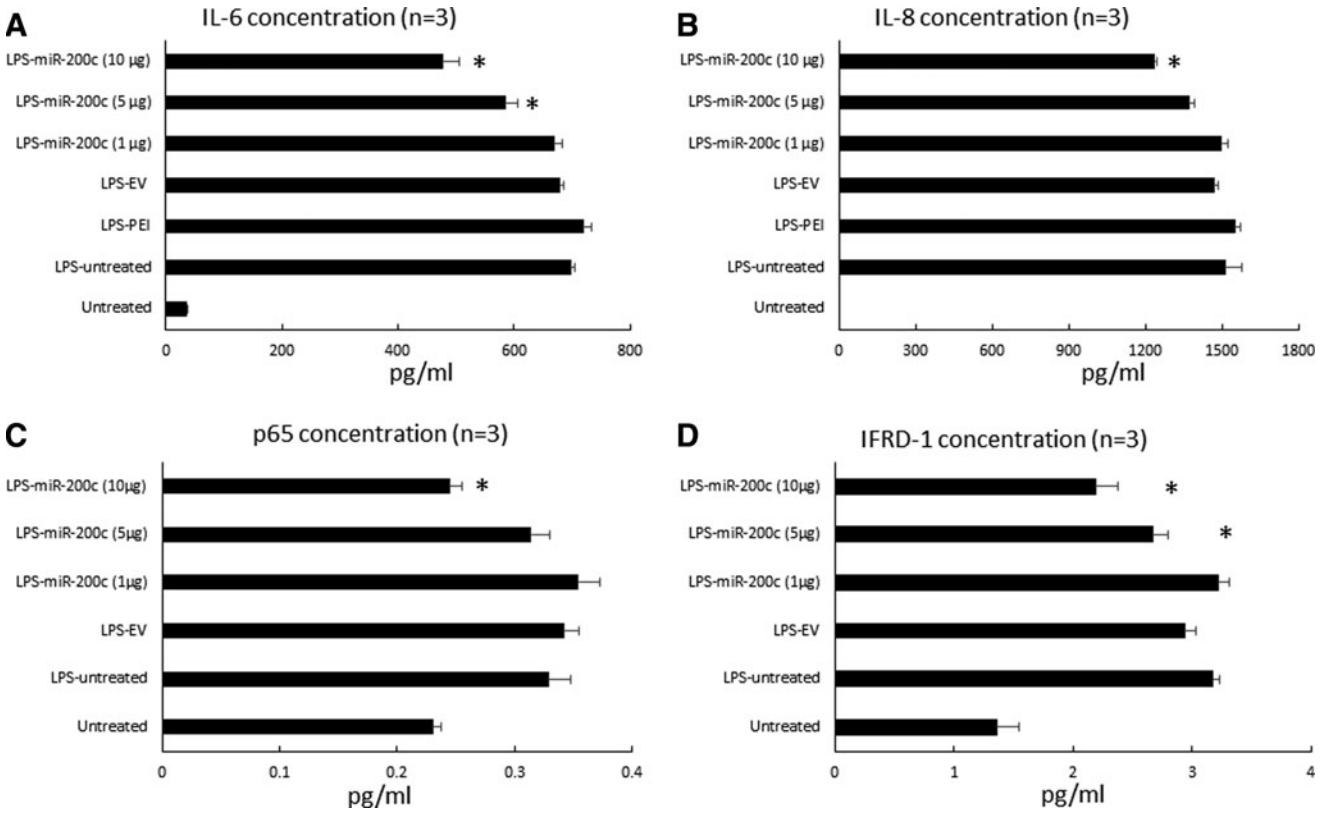

FIG. 3. *miR-200c* reduces proinflammatory and osteoclastogenic mediators after LPS stimulation. Protein concentration of *IL-6* **(A)**, *IL-8* **(B)** in the supernatant; the protein concentration of p65 **(C)** and IFRD1 **(D)** in the lysis of HGFs with different transfections 24 h after stimulation with 1 μg/mL of LPS-PG. $^*P < 0.05$ versus LPS untreated; performed in replicate.

second molar for rats receiving the LPS-PG injection than it did for sham controls. An injection of PBS and different concentrations of EV have no effect on the receding. However, rats receiving *miR-200c* treatment have less ABL. Quantitatively, the LPS injection resulted in significant ABL compared with the untreated group, as evidenced by the distance between CEJ and ABC (Fig. 5B). The distance in the groups treated with LPS with different doses of EV is similar to the group treated with LPS and with PBS. However, an LPS injection followed by treatment using *miR-200c* at 10 μg resulted in a significantly greater arrest of ABL than did PBS-treated groups ($P < 0.05$). The LPS injection also significantly increased inter-radicular space compared with sham controls ($P < 0.05$) (Fig. 5C). However, the mean inter-radicular spaces in rats treated with *miR-200c* at both 1 and 10 μg are 145 ± 12.9 μm and 131.9 ± 13.6 μm, respectively, and were significantly lower than was treatment with PBS (167.5 ± 21 μm), EV at 1 μg (179.3 ± 25.9 μm), and 10 μg (193.6 ± 16.7 μm) ($P < 0.05$). Figures 5D–G summarized the characteristics of the alveolar bone microarchitecture in LPS-injected maxillae under different treatments. The local LPS injection resulted in a decreased BV/TV (Fig. 4D) and Tb. Th (Fig. 5F), and an increased BS/BV (Fig. 5E) and total alveolar bone porosity (Fig. 5G) in rats treated with PBS or EV ($P < 0.05$). The rats treated with *miR-200c* at both 1 and 10 μg showed comparable microarchitectural parameters found in the untreated control rats. Figure 6 summarizes the histomorphometric analysis of alveolar bone resorption induced by LPS and the preventive function of local application of *miR-200c*. H&E staining showed that ACB receded more at the second molar for periodontitis rats treated with PBS than it did for sham controls (Fig. 6A). Treatment with EV has no effects on bone receding induced by LPS. However, bone resorption in the furcation area was attenuated in rats treated with a local injection of *miR-200c* at 1 and 10 μg. Quantitatively, the ratio of the remaining ACB to the root length (RL) was significantly lower in all LPS-treated rats than in the sham group ($P < 0.05$) (Fig. 6C). However, the ratio of the remaining ACB to the RL was higher for the rats treated with *miR-200c* at 1 and 10 μg (0.61 ± 0.01 and 0.61 ± 0.01, respectively,) than it was for periodontitis rats treated with PBS (0.47 ± 0.01) or EV(1 μg) (0.50 ± 0.01) ($P < 0.05$). No major morphological difference was noted between healthy controls and experimental periodontitis rats after Masson's trichrome staining (Fig. 6B). Collagen fibers at the periodontal ligament region were well individualized, but the collagen density (strong blue stain) was lower in the group of periodontitis treated with PBS.

Discussion

Our previous studies have demonstrated that *miR-200c* can effectively downregulate *IL-6, IL-8*, and *CCL-5 by* directly targeting their *3′UTRs* of and promote osteogenic differentiation of human bone marrow mesenchymal stromal

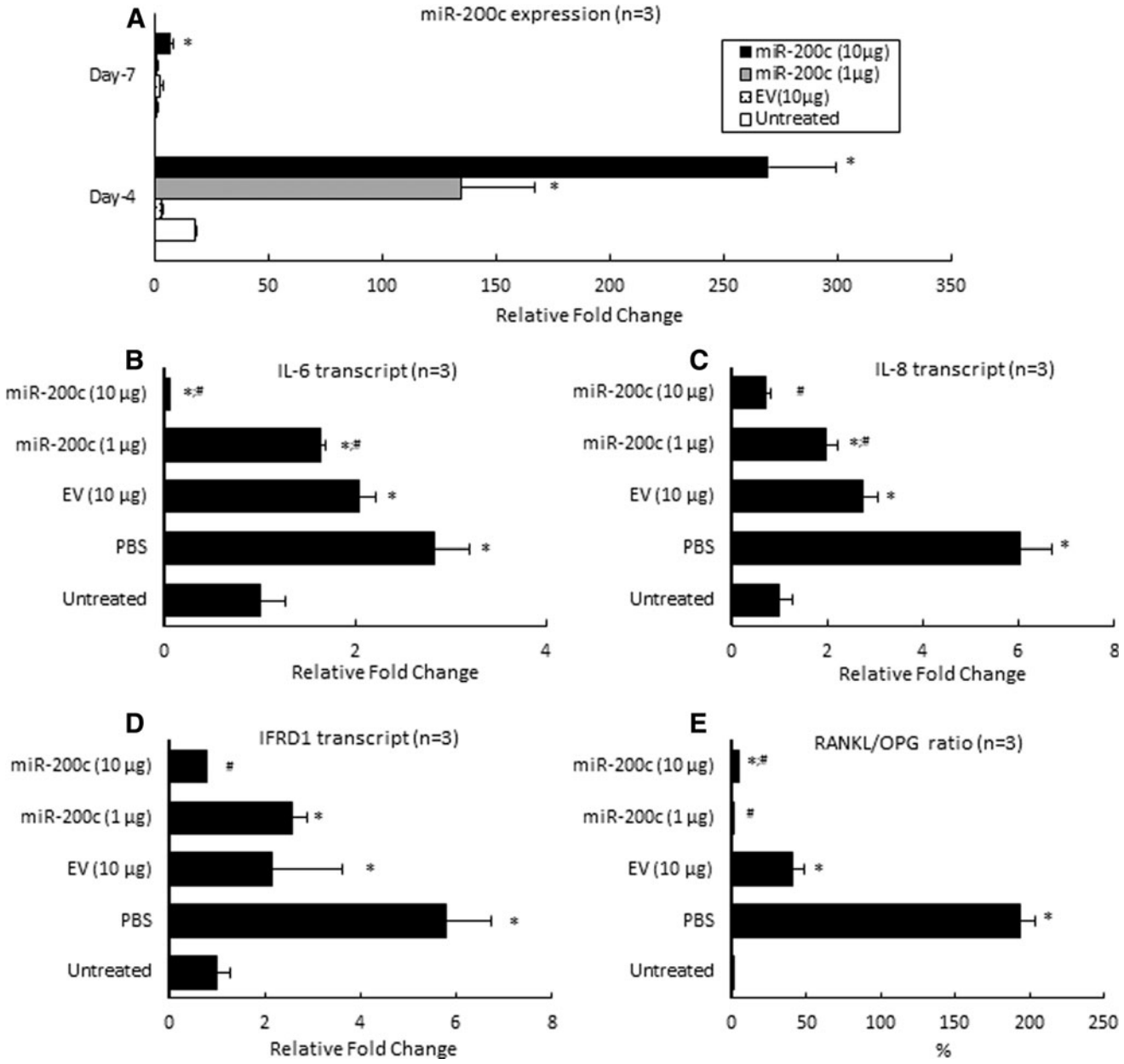

FIG. 4. *miR-200c* reduces both inflammatory and osteoclastogenic mediators in vivo. **(A)** Fold change of *miR-200c* in gingival tissue of rats 4 or 7 days after receiving PEI-*miR-200c* at 1 or 10 μg and controls. **(B–D)** Relative fold change of transcripts of *IL-6* **(B)**, *IL-8* **(C)**, *IFRD1* **(D)**, and the ratio of RANKL/OPG **(E)** at gingival tissues of rats 1 week after receiving different treatments under LPS-PG challenge at 10 μg. $^{*}P < 0.05$ versus untreated; $^{\#}P < 0.05$ versus EV; $n = 3$ for each treatment.

cells (BMSCs). In this study, we used human primary HGFs to further confirm the inhibitory function of *miR-200c* on *IL-6* and *IL-8*. We also observed that *miR-200c* increased proliferation of primary HGFs and downregulated *NF-kB* subunits (*p65* and *p50*). More importantly, we investigated, for the first time, the molecular effectiveness of *miR-200c* in inhibiting *IFRD1*, a transcription factor that plays a critical role in stimulating osteoclastogenesis and inhibiting bone formation [31,32]. With bioinformatic analysis we predicted that *miR-200c* may directly target the *3′UTR* of IFRD1. In this study, the inhibitory functions of *miR-200*c on these proinflammatory and osteoclastogenic mediators were also confirmed in vivo after a local injection of *miR-200c* at rat gingiva. In addition, in the rat model of periodontitis, we demonstrated that, for the first time, local application of *miR-200c* could effectively arrest ABL induced by LPS, including reducing the distance of ABC to CEJ and the inter-radicular space and restoring microarchitecture of the alveolar bone. These results strongly suggested that *miR-200c* may serve as an effective inhibitor of multiple proinflammatory and osteoclastogenic mediators to treat chronic periodontitis (Fig. 7).

In this study, we demonstrated that PEI effectively delivered *miR-200c* into primary HGFs in vitro, and the

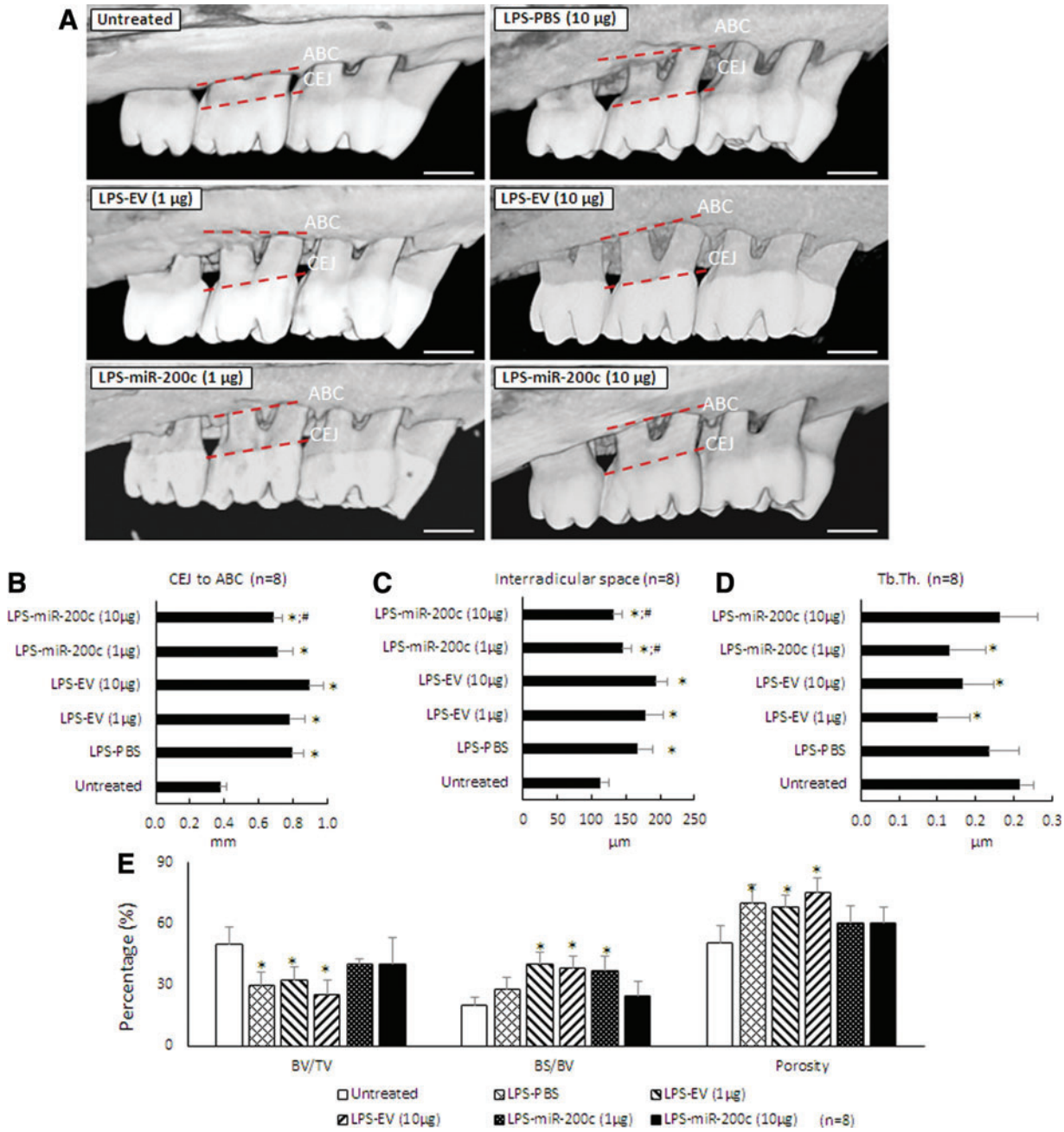

FIG. 5. *miR-200c* protects LPS-induced ABL in rat periodontitis. Rats were injected bi-weekly with 10 μg LPS and treated weekly with one injection of PBS, PEI facilitating EV (1 and 10 μg), *miR-200c* (1 and 10 μg) up to 4 weeks. **(A)** Three-dimensional reconstructed micro-computed tomography images of maxillary alveolar bone on the palatal sides of rats 4 weeks after receiving an LPS injection with and without *miR-200c*. *Red dot lines* indicate the ABC and CEJ at maxillary second molars. Scale bars: 1 mm. **(B, C)** The outcome of the ABL **(B)** and the inter-radicular space **(C)** at the M2 after 4 weeks. **(D, E)** Structural parameters of alveolar bone 4 weeks after different treatment, including (Tb. Th) **(D)**, and the percentages of BV/TV, BS/BV, and the total alveolar bone porosity **(E)**. $^{*}P < 0.05$ versus untreated; $^{\#}P < 0.05$ versus LPS-PBS; $n = 8$ for each treatment. ABC, alveolar bone crest; ABL, alveolar bone loss; BS, bone surface; BV, bone volume; CEJ, cemento-enamel junction; M2, second maxillary molar; PBS, phosphate-buffered saline; Tb. Th, trabecular thickness; TV, tissue volume. Color images are available online.

transfection efficiency was dose dependent. This result was similar to the transfection into human periodontal ligament fibroblasts and bone marrow mesenchymal stromal cells [24,33]. We also demonstrated, for the first time, that PEI effectively facilitated the in vivo transfection of pDNA encoding *miR-200c* into rat gingiva by a local injection. For PEI-*miR-200c* nanoplex treatment in vivo, we also observed that the upregulated content of *miR-200c* expression was dose dependent, which provides the capability to optimize the effects of *miR-200c* by controlling the PEI-*miR-200c* nanoplex concentration and *miR-200c* expression level. Although the transfection efficiency mediated by PEI was

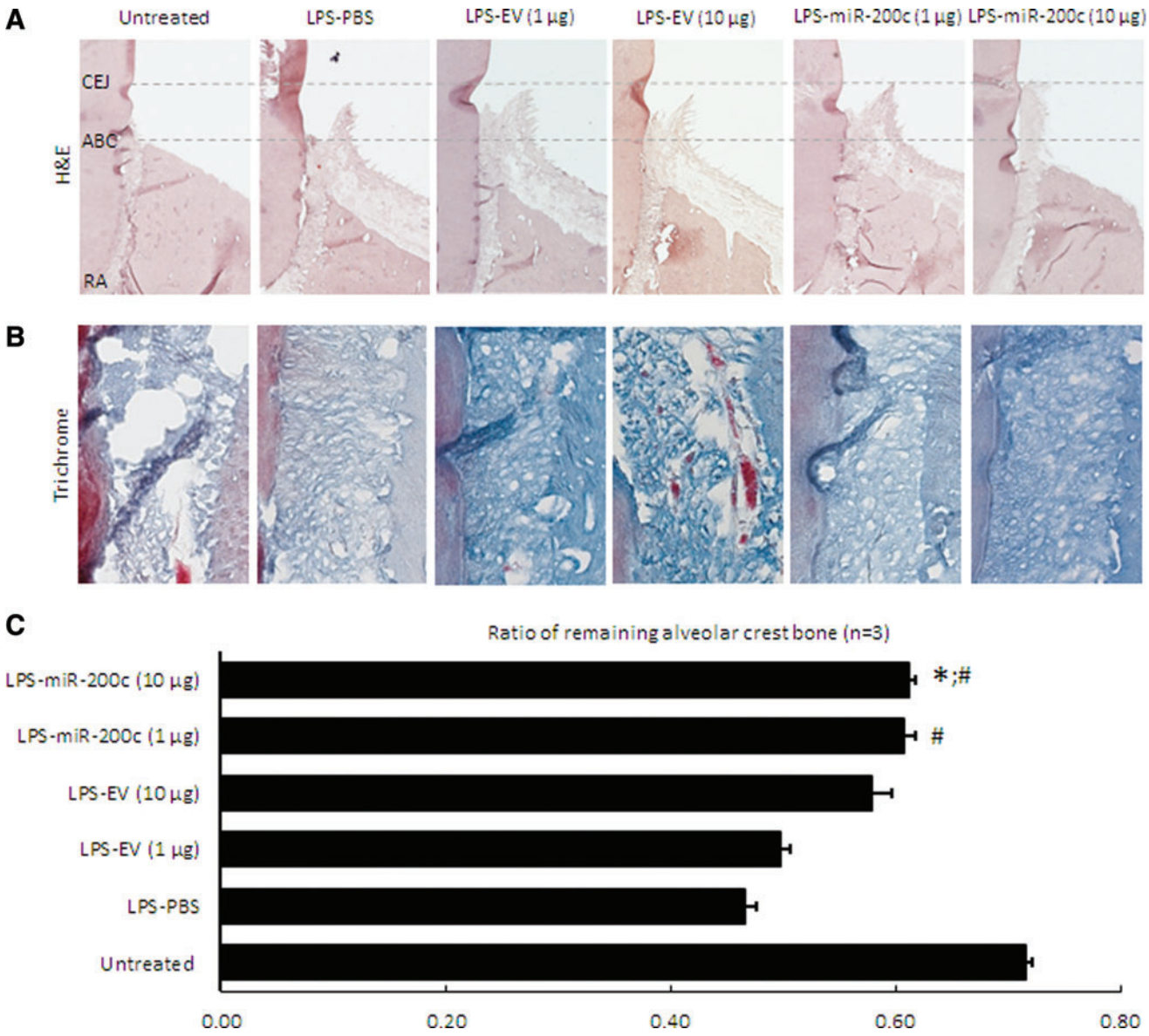

FIG. 6. Histological analysis of alveolar bone and periodontal ligament adjacent to the M2 of 4 weeks LPS-treated rats. **(A)** and **(B)** Representative micrographs of sham and periodontitis rats treated with PBS, PEI facilitating EV (1 and 10 μg), and *miR-200c* (1 and 10 μg) with hematoxylin and eosin staining **(A)** and Masson's trichrome staining **(B)**. Magnification = 4. **(C)** Ratio of the remaining ACB to the RL adjacent to the M2. The ratio of the ACB to the RL was calculated by using the formula (ABC-RA)/(CEJ-RA), where ABC-RA is the distance from ABC to RA and CEJ-RA is the distance from CEJ to RA. $*P < 0.05$ vs untreated; $^{\#}P < 0.05$ versus LPS-PBS; $n = 3$ for each treatment. ACB, alveolar crest bone; RA, root apex; RL, root length. Color images are available online.

associated with dose-dependent cytotoxicity and apoptosis in previous studies [33,34], we did not observe significant toxicity from PEI that mediated the transfection of *miR-200c* in this study. Further, we observed that PEI had certain effects, including a reduction of *IFRD1, p65*, and *p50*, which indicated that, for the first time, PEI might have inhibitory effectiveness on the *NF-kB* pathway. Although *NF-kB* was considered to be involved in PEI-induced apoptosis, more studies are needed to understand the molecular function and underlying mechanism(s) of PEI on *NF-kB* signal activity. In addition, although PEI effectively facilitated the transfection of pDNA *miR-200c*, the overexpression of *miR-200c* lasted a relatively short period (about a week). To effectively develop *miR-200c* for clinical application, sustained release of *miR-200c* to maintain an optimal overexpression of *miR-200c* is needed. In this study, we also observed that the cellular inflammation response was slightly mediated by EV. Transfection of EV increased cellular inflammatory reaction, including upregulated *IL-6* and *p50*. Although the mechanism(s) are not clear, they are probably caused by the innate immune system of the cells that can recognize nucleic acids after transfection [35].

In this study, a strong and dose-dependent inhibitory effect of *miR-200c* on proinflammatory cytokines was observed both in vitro and in vivo. However, the effectiveness to prevent bone resorption required a relatively high dose of

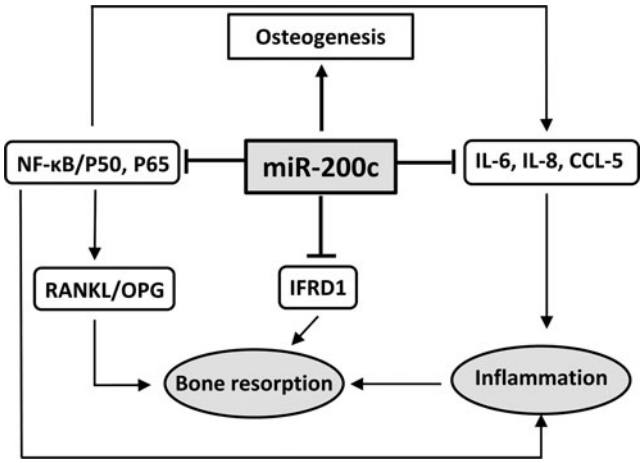

FIG. 7. Potential mechanism(s) of anti-inflammatory/osteoclastogenic function of *miR-200c* to attenuate periodontitis.

miR-200c. In addition, compared with the normal untreated control, we found that even with a high dose of *miR-200c* significant periodontal bone loss occurred under the LPS challenge, which indicated that *miR-200c* did not completely block ABL in this periodontitis model. Many factors may contribute to these findings, including a relatively high dose of LPS applied in the rat model of periodontitis, uneven distribution of *miR-200c* and its infiltration into the inflammatory periodontal tissues, and the local inflammation caused by frequent injections into the gingiva. Therefore, other animal models characterized with chronical periodontitis may be needed to further prove the therapeutic effect of *miR-200c* on periodontitis. Other specific miRs that can synergize the inhibitory function of *miR-200c* on inflammation and osteoclastogenesis may also be needed in future studies. In this study, we demonstrated that *miR-200c* reduced proinflammatory cytokines and osteoclastogenic mediators to attenuate periodontitis; however, it lacks inhibitory effects of *miR-200c* directly on osteoclasts. We will continue to investigate whether *miR-200c* and other miRs have direct functions to target osteoclast activity both in vitro and in vivo.

Acknowledgments

The authors thank Dr. J. Michael Tilley for proofreading and editing the article. This study was supported by the National Institute of Dental and Craniofacial Research (grant nos. R21 DE024799, R21 DE025328, and R01 DE026433) of the National Institutes of Health (NIH). M.R.-B. would like to acknowledge the support received from the NIH under the R90 DE024296-03 grant to pursue a career in dental science.

Author Disclosure Statement

No competing financial interests exist.

References

1. Eke PI, BA Dye, L Wei, GO Thornton-Evans, RJ Genco and Cdc Periodontal Disease Surveillance workgroup: James Beck GDRP. (2012). Prevalence of periodontitis in adults in the United States: 2009 and 2010. J Dent Res 91: 914–920.
2. Muller HP and M Ulbrich. (2005). Alveolar bone levels in adults as assessed on panoramic radiographs. (I) Prevalence, extent, and severity of even and angular bone loss. Clin Oral Investig 9:98–104.
3. Sanz M, A Ceriello, M Buysschaert, I Chapple, RT Demmer, F Graziani, D Herrera, S Jepsen, L Lione, et al. (2018). Scientific evidence on the links between periodontal diseases and diabetes: consensus report and guidelines of the joint workshop on periodontal diseases and diabetes by the International diabetes Federation and the European Federation of Periodontology. Diabetes Res Clin Pract 137: 231–241.
4. Armas J, S Culshaw, L Savarrio. (2013). Treatment of periimplant diseases: a review of the literature and protocol proposal. Dent Update 40: 472–480.
5. Papapanou PN and MS Tonetti. (2000). Diagnosis and epidemiology of periodontal osseous lesions. Periodontol 22:8–21.
6. Sidiropoulou-Chatzigiannis S, M Kourtidou and Tsalikis. (2007). The effect of osteoporosis on periodontal status, alveolar bone and orthodontic tooth movement. A literature review. J Int Acad Periodontol 9:77–84.
7. Khosla S, JP Bilezikian, DW Dempster, EM Lewiecki, PD Miller, RM Neer, RR Recker, E Shane, D Shoback and JT Potts. (2012). Benefits and risks of bisphosphonate therapy for osteoporosis. J Clin Endocrinol Metab 97(7) 2272–2282.
8. Urade M. (2007). Bisphosphonates and osteonecrosis of the jaws. Clin Calcium 17:241–248.
9. Di Benedetto A, I Gigante, S Colucci and M Grano. (2013). Periodontal disease: linking the primary inflammation to bone loss. Clin Dev Immunol 2013:503754.
10. Darveau RP. (2010). Periodontitis: a polymicrobial disruption of host homeostasis. Nat Rev Microbiol 8:481–490.
11. Herath TD, RP Darveau, CJ Seneviratne, CY Wang, Y Wang and L Jin. (2013). Tetra- and penta-acylated lipid A structures of *Porphyromonas gingivalis* LPS differentially activate TLR4-mediated NF-kappaB signal transduction cascade and immuno-inflammatory response in human gingival fibroblasts. PLoS One 8:e58496.
12. Graves DT, T Oates and GP Garlet. (2011). Review of osteoimmunology and the host response in endodontic and periodontal lesions. J Oral Microbiol 3:10.3402.
13. Mogi M, Otogoto J, Ota N and Togari A. (2004). Differential expression of RANKL and osteoprotegerin in gingival crevicular fluid of patients with periodontitis. J Dent Res 83:166–169.
14. Jain S and RP Darveau. (2010). Contribution of *Porphyromonas gingivalis* lipopolysaccharide to periodontitis. Periodontol 54:53–70.
15. Mao CY, YG Wang, X Zhang, XY Zheng, TT Tang and EY Lu. (2016). Double-edged-sword effect of IL-1beta on the osteogenesis of periodontal ligament stem cells via crosstalk between the NF-kappaB, MAPK and BMP/Smad signaling pathways. Cell Death Dis 7:e2296.
16. Singh RP, I Massachi, S Manickavel, S Singh, NP Rao, S Hasan, DK Mc Curdy, S Sharma, D Wong, BH Hahn, H Rehimi. (2013). The role of miRNA in inflammation and autoimmunity. Autoimmun Rev 12:1160–1165.
17. Stoecklin-Wasmer C, P Guarnieri, R Celenti, RT Demmer, M Kebschull and PN Papapanou. (2012). MicroRNAs and

their target genes in gingival tissues. J Dent Res 91(10): 934–940.
18. Venugopal P, T Koshy, V Lavu, S Ranga Rao, S Ramasamy, S Hariharan and V Venkatesan. (2018). Differential expression of microRNAs let-7a, miR-125b, miR-100, and miR-21 and interaction with NF-kB pathway genes in periodontitis pathogenesis. J Cell Physiol 233:5877–5884.
19. Katoh Y and M Katoh. (2008). Hedgehog signaling, epithelial-to-mesenchymal transition and miRNA (review). Int J Mol Med 22:271–275.
20. Rokavec M, W Wu and JL Luo. (2012). IL6-mediated suppression of miR-200c directs constitutive activation of inflammatory signaling circuit driving transformation and tumorigenesis. Mol Cell 45:777–789.
21. Wendlandt EB, JW Graff, TL Gioannini, AP McCaffrey and ME Wilson. (2012). The role of MicroRNAs miR-200b and miR-200c in TLR4 signaling and NF-kappa B activation. Innate Immun 18:846–855.
22. Howe EN, DR Cochrane, DM Cittelly, JK Richer. (2012). miR-200c targets a NF-kappa B up-regulated TrkB/NTF3 autocrine signaling loop to enhance anoikis sensitivity in triple negative breast cancer. PLoS One 7(11):e49987.
23. Kumar S, A Nag and CC Mandal. (2015). A comprehensive review on miR-200c, a promising cancer biomarker with therapeutic potential. Curr Drug Targets 16:1381–1403.
24. Hong L, T Sharp, B Khorsand, C Fischer, S Eliason, A Salem, A Akkouch, K Brogden and BA Amendt. (2016). MicroRNA-200c represses IL-6, IL-8, and CCL-5 expression and enhances osteogenic differentiation. PLoS One 11(8):e0169381.
25. Dumitrescu AL, S Abd-El-Aleem, B Morales-Aza and LF Donaldson. (2004). A model of periodontitis in the rat: effect of lipopolysaccharide on bone resorption, osteoclast activity, and local peptidergic innervation. J Clin Periodontol 31:596–603.
26. Souza JAC, AVB Nogueira, PPC Souza, G Oliveira, MC Medeiros, GP Garlet, JA Cirelli and CJ Rossa. (2017). Suppressor of cytokine signaling 1 expression during LPS-induced inflammation and bone loss in rats. Braz Oral Res 31:e75.
27. Intra J and AK Salem. (2008). Characterization of the transgene expression generated by branched and linear polyethylenimine-plasmid DNA nanoparticles in vitro and after intraperitoneal injection in vivo. J Control Release 130:129–138.
28. Nagasawa T, H Kobayashi, M Kiji, M Aramaki, R Mahanonda, T Kojima, Y Murakami, M Saito, Y Morotome and I Ishikawa. (2002). LPS-stimulated human gingival fibroblasts inhibit the differentiation of monocytes into osteoclasts through the production of osteoprotegerin. Clin Exp Immunol 130:338–344.
29. Eisenberg E and EY Levanon. (2013). Human housekeeping genes, revisited. Trends Genet 29:569–574.
30. Kozera B and M Rapacz, (2013). Reference genes in real-time PCR. J Appl Genet 54:391–406.
31. Iezaki T, K Fukasawa, G Park, T Horie, T Kanayama, K Ozaki, Y Onishi, Y Takahata, Y Nakamura, et al. (2016). Transcriptional modulator Ifrd1 regulates osteoclast differentiation through enhancing the NF-kappaB/NFATc1 pathway. Mol Cell Biol 36:2451–2463.
32. Xie Z, H Yu, X Sun, P Tang, Z Jie, S Chen, J Wang, A Qin and S Fan. (2018). A novel diterpenoid suppresses osteoclastogenesis and promotes osteogenesis by inhibiting Ifrd1-mediated and IkappaBalpha-mediated p65 nuclear translocation. J Bone Miner Res 33:667–678.
33. Atluri K, D Seabold, L Hong, S Elangovan and AK Salem. (2015). Nanoplex-mediated codelivery of fibroblast growth factor and bone morphogenetic protein genes promotes osteogenesis in human adipocyte-derived mesenchymal stem cells. Mol Pharm 12:3032–3042.
34. Pishavar E, M Shafiei, S Mehri, M Ramezani and K Abnous. (2017). The effects of polyethylenimine/DNA nanoparticle on transcript levels of apoptosis-related genes. Drug Chem Toxicol 40:406–409.
35. Atianand MK and KA Fitzgerald. (2013). Molecular basis of DNA recognition in the immune system. J Immunol 190: 1911–1918.

Address correspondence to:
Dr. Liu Hong
Iowa Institute for Oral Health Research
College of Dentistry
The University of Iowa
801 Newton Avenue
Iowa City, IA

E-mail: liu-hong@uiowa.edu

Received for publication February 11, 2019
Accepted after revision April 22, 2019
Prepublished on Liebert Instant Online April 24, 2019